MCB
Journals.ASM.org

Constitutive Notch Activation Upregulates Pax7 and Promotes the Self-Renewal of Skeletal Muscle Satellite Cells

Yefei Wen,[a] Pengpeng Bi,[a] Weiyi Liu,[a] Atsushi Asakura,[b] Charles Keller,[c] and Shihuan Kuang[a,d]

Department of Animal Sciences, Purdue University, West Lafayette, Indiana, USA[a]; Stem Cell Institute, Paul and Sheila Wellstone Muscular Dystrophy Center, and Department of Neurology, University of Minnesota Medical School, Minneapolis, Minnesota, USA[b]; Pediatric Cancer Biology Program, Papé Family Pediatric Research Institute, Department of Pediatrics, Oregon Health and Science University, Portland, Oregon, USA[c]; and Purdue University Center for Cancer Research, West Lafayette, Indiana, USA[d]

Notch signaling is a conserved cell fate regulator during development and postnatal tissue regeneration. Using skeletal muscle satellite cells as a model and through myogenic cell lineage-specific NICD^{OE} (overexpression of constitutively activated Notch 1 intracellular domain), here we investigate how Notch signaling regulates the cell fate choice of muscle stem cells. We show that in addition to inhibiting MyoD and myogenic differentiation, NICD^{OE} upregulates Pax7 and promotes the self-renewal of satellite cell-derived primary myoblasts in culture. Using MyoD$^{-/-}$ myoblasts, we further show that NICD^{OE} upregulates Pax7 independently of MyoD inhibition. In striking contrast to previous observations, NICD^{OE} also inhibits S-phase entry and Ki67 expression and thus reduces the proliferation of primary myoblasts. Overexpression of canonical Notch target genes mimics the inhibitory effects of NICD^{OE} on *MyoD* and *Ki67* but not the stimulatory effect on *Pax7*. Instead, NICD regulates *Pax7* through interaction with RBP-Jκ, which binds to two consensus sites upstream of the *Pax7* gene. Importantly, satellite cell-specific NICD^{OE} results in impaired regeneration of skeletal muscles along with increased Pax7^{+} mononuclear cells. Our results establish a role of Notch signaling in actively promoting the self-renewal of muscle stem cells through direct regulation of *Pax7*.

Skeletal muscles can efficiently regenerate after injury. This remarkable regenerative capacity requires the contribution of a population of muscle resident stem cells called satellite cells (27, 29, 42). Pax7 expression is crucial for the embryonic specification, survival, and maintenance of the satellite cell lineage (22, 26, 35, 39, 46). In mature resting muscles, satellite cells are predominantly quiescent. Upon muscle injury, satellite cells are activated, enter the cell cycle, and proliferate. The proliferating satellite cells, called myoblasts, subsequently withdraw from the cell cycle to either differentiate or self-renew. The quiescent, proliferating, self-renewing, and differentiating satellite cells can be readily distinguished by the expression of several transcription factors, i.e., Pax7^{+}, Pax7^{+} MyoD^{+}, Pax7^{+} MyoD^{-}, and Pax7^{-} MyoD^{+} myogenin^{+}, respectively (16, 32, 55). However, the signaling pathways that actively maintain/suppress satellite cells in these different states are not well understood.

The Notch signaling pathway plays critical roles in cell-cell communication and cell fate regulation during tissue morphogenesis, homeostasis, and regeneration (20). In vertebrates, Notch signaling is initiated by extracellular ligands (Dll1, -3, and -4 and Jag1 and -2) that interact with Notch1 to -4 receptors, leading to sequential cleavage of Notch extracellular and intracellular domains. Once cleaved, the Notch intracellular domain (NICD) translocates to the nucleus, where it interacts with RBP-Jκ (also called CBF1) and activates the transcription of specific target genes, including *Hes* and *Hey* family genes. During embryonic muscle development (myogenesis), oscillatory Notch activity defines the anterior boundary of somites and progenitor cell fate within the somites (17, 18, 38). Notch signaling further inhibits the myogenic differentiation of embryonic progenitors (12). Disruption of Notch signaling through *Dll1* or *RBP-Jκ* mutation leads to premature differentiation of myogenic precursors and depletion of satellite cells (44, 50).

Notch signaling is also critical for postnatal myogenesis (muscle regeneration). Notch signaling is activated upon muscle injury, and reduced Notch activation has been associated with defective muscle regeneration in aged muscles (8, 9). Sarcopenia, a common aging-associated muscle wasting condition, is thought to be at least partially due to reduced satellite cell activity. Intriguingly, activation of the Notch signaling pathway by intramuscular injection of a Notch1 antibody rescued the regenerative defects of aged muscles, whereas blockage of Notch signaling via a diffusible ligand for Notch receptors led to defective regeneration of young muscles (8). Furthermore, exposure of aged muscle to a younger systemic environment by parabiotic pairing restored the ability of aged muscles to activate Notch signaling and to efficiently regenerate (9). As both focal and systemic manipulation of Notch signaling can in principle target all cell types in muscle, including satellite cells, myofibers, nerve- and blood vessel-associated cells, as well as other interstitial cells, whether satellite cell-specific activation of Notch signaling enhances the regeneration of injured muscles remains unclear.

Notch signaling has been shown to play various roles in the quiescence/activation, proliferation, and differentiation of satellite cells and myogenic C2C12 cells. Notch signaling regulates the asymmetric cell fate segregation in newly divided satellite daugh-

Received 20 December 2011 **Returned for modification** 6 January 2012
Accepted 30 March 2012
Published ahead of print 9 April 2012
Address correspondence to Shihuan Kuang, skuang@purdue.edu.
Supplemental material for this article may be found at http://mcb.asm.org/.

doi:10.1128/MCB.06753-11

ter cells (10, 23, 47). The committed daughter cell expresses elevated Dll1, which presumably initiates Notch signaling in the neighboring sister cell that undergoes self-renewal (23). Likewise, Numb, a Notch inhibitor, is specifically expressed in the daughter cell that differentiates (10). Consistently, activation of Notch signaling or overexpression of Notch target genes in C2C12 myoblasts markedly inhibits *MyoD*, *Myogenin*, and *Mef2c* expression and myogenic differentiation (4, 21, 24, 25, 54). Other studies have indicated that Notch signaling promotes satellite cell activation and proliferation (8, 10). Satellite cells isolated from aged muscles exhibited delayed activation and reduced proliferation kinetics due to deficient upregulation of Notch signaling (8). In contrast, activation of Notch signaling in cultured myoblasts enhanced their proliferation (8, 9). However, two recent studies demonstrated that Notch signaling is necessary for maintaining satellite cell quiescence, as conditional knockout of *RBP-Jκ* in satellite cells resulted in spontaneous activation and differentiation of satellite cells (2, 28). One way to address some of the conflicting observations awaits techniques to constitutively activate Notch signaling specifically in satellite cells.

Notch's effects on satellite cells can be modulated by both micro- and systemic environments. For example, matrix heparan sulfate proteoglycans Syndecan 3 and Syndecan 4 regulate the self-renewal, proliferation, and differentiation of satellite cells through modulating Notch signaling (11, 13, 48). Loss of Syndecan 3 leads to reduced expression of Notch target genes due to defective ADAM17/TACE-mediated S2 cleavage and γ-secretase-mediated S3 cleavage in Notch processing (37). More recently, it has been shown that Dll1 expressed by neural crest progenitors migrating *en route* through embryonic somites transiently activates Notch signaling in myogenic progenitors and promotes myogenic differentiation (40). Notch signaling may also be modulated by environmental oxygen levels, as HIF1a functionally interacts with NICD (15). Lastly, systemic WNT and transforming growth factor β (TGF-β) signaling and also tumor necrosis factor alpha released by injured myofibers have been shown to antagonize Notch signaling in myogenic satellite cells (1, 3, 6).

To date, whether Notch signaling actively regulates the self-renewal (rather than doing so by passively repressing differentiation) of satellite cells has not been known. In the present study, we address this question through genetic gain-of-function studies. We show that constitutive activation of Notch signaling in myogenic progenitors results in decreased proliferation and differentiation but increased self-renewing of progenitor cells. Consistently, *de novo* activation of Notch signaling upregulated Pax7 expression in culture and inhibited muscle regeneration *in vivo*. Target gene profiling and functional analysis suggested that canonical Notch targets mediate the functional output of Notch activation on proliferation and differentiation, and NICD directly regulates *Pax7* to enhance self-renewal. These results provide mechanistic insights into how Notch signaling regulates skeletal muscle development and homeostasis.

MATERIALS AND METHODS

Mice and animal care. *ROSA26-N1ICD* mice were obtained from Jackson Laboratories (stock number 008159; Bar Harbor, ME) (30). *Pax7-Cre*^{ER} mice were constructed by insertion of an internal ribosome entry site-Cre^{ER} fragment at the 3′ end of the endogenous *Pax7* gene (31). Mouse maintenance and experimental use were performed according to protocols approved by the Purdue Animal Care and Use Committee.

RNA isolation and quantitative pCR (qPCR) analysis. Tissue samples for RNA were excised after euthanasia and either stored in RNAlater (Ambion, Woodlands, TX) for later processing or homogenized immediately for RNA purification by using the Qiagen RNeasy fibrous tissue minikit (Qiagen, Inc., Valencia, CA). Myoblasts were lysed in RNAlater for RNA purification using the Qiagen RNeasy minikit (Qiagen, Inc., Valencia, CA). An on-column DNase I digestion set (Sigma-Aldrich, St. Louis, MO) was used to remove any trace amounts of genomic DNA. Purified RNA samples were then quantified by using a NanoDrop 1000 apparatus (Wilmington, DE). Equal amounts of RNA were reverse transcribed using random hexamer primers and Moloney murine leukemia virus reverse transcriptase (Invitrogen, Inc., Carlsbad, CA).

Quantitative PCR was performed using the Roche LightCycler 480 system with SYBR green master mix reagents (Roche Applied Science, Indianapolis, IN). Samples were assayed in duplicate with cDNA reverse transcribed from 10 ng of RNA in 10-μl PCR mixtures. The genes for ribosomal protein large protein 38 (*Rplp38*), glyceraldehyde-3-phosphate dehydrogenase (*Gapdh*), and β-actin were used as the housekeeping gene controls for ΔC_T calculations [ΔC_T = (C_T of the target gene) − (average C_T of housekeeping genes)]. Primer sequences and PCR conditions are listed in Table S2 of the supplemental material. Fold expression values were calculated using the $2^{-\Delta\Delta CT}$ method, where $\Delta\Delta C_T$ = (ΔC_T of the treatment sample) − (ΔC_T of control samples) (with the control value normalized to 1). Statistical significance was determined by analysis of variance.

Western blotting. Expressional levels of proteins were determined by Western blot analysis. Briefly, myoblasts attached to plates were rinsed with ice-cold phosphate-buffered saline (PBS), and cells were scraped on ice in radioimmunoprecipitation assay (RIPA) buffer (50 mM Tris-Cl [pH 8.0], 200 mM NaCl, 50 mM NaF, 1 mM dithiothreitol, 1 mM Na_3VO_4, 0.3% IGEPAL, and protease inhibitor cocktail). Cells were collected in 1.5-ml Eppendorf tubes, lysed on ice for 30 min, and centrifuged at 15,000 rpm for 10 min at 4°C to removed cell debris. Tissue samples were homogenized in RIPA buffer, lysed, and centrifuged in similar ways. Protein concentrations were quantified with bicinchoninic acid reagent, and 30-μg protein samples were loaded in each lane onto 10-to-12% SDS-PAGE gels. Electrophoresis, electrotransfer of proteins to polyvinylidene difluoride membranes, and antibody staining were conducted following standard procedures previously described (51). The antibodies used are listed in Table S1 of the supplemental material. Antibody-labeled protein bands were revealed by using the RapidStep enhanced chemiluminescence reagent (Calbiochem) and detected with the GEL Logic 2200 imaging system (Carestream Health Inc.).

Muscle injury and regeneration. Muscle regeneration was induced by injections of cardiotoxin (CTX; Sigma-Aldrich, St. Louis, MO) into the tibialis anterior (TA) muscle. Mice were anesthetized using a ketamine-xylazine cocktail, and then 50 μl of 10 μM CTX was injected into the left TA muscle. Muscles were then harvested at 7 and 21 days postinjection to assess the completion of regeneration and repair.

Muscle cryosectioning and staining. Fresh or fixed TA muscles were embedded in OCT compound and frozen in isopentane chilled on a dry ice-ethanol slurry. For fixation, muscles were placed in 4% paraformaldehyde (PFA) for 1 h, washed in 100 mM glycine for 1 h, and then sunk in 30% sucrose at 4°C overnight. Frozen muscles were cut into 10-μm-thick cross-sections by using a Leica CM1850 cryostat.

Immunofluorescence staining of muscle sections was performed as previously described (22) using the antibodies listed in Table S1 of the supplemental material. Fluorescent images were captured with a CoolSnap HQ charge-coupled-device camera (Photometrics) driven by IP Lab software (Scanalytics Inc.) using a Leica DM6000 microscope with a 20× objective (numerical aperture, 0.70). Single-channel black-and-white fluorescent images were assembled into multicolor images with the Photoshop software. Hematoxylin and eosin (H&E)-stained images were captured with a Nikon D90 digital camera installed on a Nikon (Diaphot) inverted microscope. The cross-sectional area (CSA) of myofibers was

analyzed with the Image Analysis Tool in Photoshop. Specifically, the CSA was calculated as the total myofiber area divided by the number of myofibers.

Culture and staining of single myofibers and primary myoblasts. Single myofibers were isolated from the extensor digitorum longus (EDL) muscles after digestion with collagenase A (Sigma) and trituration as previously described (7, 41). Suspended fibers were cultured in 60-mm horse serum-coated plates in Dulbecco's modified Eagle's medium supplemented with 10% fetal bovine serum (FBS; HyClone, Logan, UT), 2% chicken embryo extract (Accurate Chemical, Westbury, NY), and 1% penicillin-streptomycin for 3 days. Freshly isolated fibers and cultured fibers were then fixed in 4% PFA and stained for Pax7, MyoD, and green fluorescent protein (GFP) as previously described (22).

Primary myoblasts were isolated from hind limb skeletal muscle. Muscles were minced and digested in type I collagenase and Dispase B mixture (Roche Applied Science). Cells were then filtered from debris, centrifuged, and cultured in growth medium (F-10 Ham's medium supplemented with 20% FBS, 4 ng/ml basic fibroblast growth factor, and 1% penicillin-streptomycin) on collagen-coated cell culture plates at 37°C, 5% CO_2, as previously described (51).

Viral and electroporation-mediated gene transfer. Notch target genes *Hes5*, *HeyL*, and *Nrarpa* were cloned from myoblast cDNA with restriction enzyme sites at each terminal and then were ligated to pCMV-2b plasmids. *Hes1*, *Hes6*, and *Hey1* were subcloned from plasmids purchased from Open Biosystems (Thermo Fisher Scientific, Huntsville, AL) to pCMV-2b plasmids separately. The pPGK-Cre-bpA plasmid was obtained from Addgene (Cambridge, MA).

Adenovirus containing *Cre-EGFP* or *EGFP* (generously provided by Y.-X. Wang, University of Massachusetts) was used to activate N1ICD in primary myoblasts isolated from ROSA-N1ICD mice. Adenovirus infection was performed when myoblasts reached 50 to 80% confluence. Myoblasts in plates were washed in PBS 3 times, and then adenovirus diluted in Ham's F-10 was added. The Ham's F-10 medium was replaced with fresh growth medium and plates were returned to the incubator for 30 to 60 min. Virus titers were determined in myoblasts by scoring GFP-positive cells (36). Adenovirus-infected myoblasts were harvested at 24 h for RNA and protein extraction.

Lentivirus-mediated shRNA knockdown. An shRNA set targeting *RBP-Jκ* was purchased from Open Biosystems (Thermo Fisher Scientific, Huntsville, AL) and packaged into lentiviral particles in 293T cells together with lentiviral envelope plasmids. Supernatant was removed and replaced with fresh medium after 24 h. In another 24 h, supernatant was collected and centrifuged to remove the cells and debris (3,000 rpm, 5 min). Equal volumes of lentiviral supernatant were mixed with fresh myoblast growth medium and added to the cultured primary myoblasts. Myoblasts were harvested at 48 h for isolation of DNA, RNA, and protein.

Electroporation-mediated transfection was performed on primary myoblasts by using a Neon transfection system (Invitrogen) as previously described (51). Briefly, 1×10^5 cells were suspended in 10 μl electroporation buffer, including 2.5 μg plasmids containing Notch target genes, and electroporated (1,300 V, 10 ms, 3 times), using a 10-μl tip. After electroporation, the cells were cultured in 6-well plates. In 24 h, the cells were harvested for RNA purification.

Cell growth rate and 5-bromodeoxyuridine (BrdU) incorporation analysis. Primary myoblasts were seeded in 6-well plates (1×10^5 cells/well) and cultured under standard myoblast conditions (see above). The cells were harvested at days 2, 4, 6, 10, and 12 and counted by using a hemocytometer.

A BrdU incorporation assay was employed to determine the proliferation of myoblasts. Myoblasts were cultured in 4- or 8-well chamber slides. At 70% confluence, BrdU was added to the medium at a 60 μM final concentration. Cells were fixed in 4% PFA after 24 h and incubated in HCl (1 M) for 10 min on ice, followed by HCl (2 M) for 10 min at room temperature (RT). Borate buffer was added to neutralize the cells. BrdU staining was performed, followed by GFP, Pax7, and MyoD staining.

Chromotin immunoprecipitation. Proliferating primary myoblasts and C2C12 myoblasts were cross-linked with 1% formaldehyde in Ham's F-10 medium for 10 min at RT followed by the addition of 125 mM glycine for 5 min at RT, after which cells were scraped into SDS lysis buffer. The cells were further sonicated and diluted for immunoprecipitation with the indicated antibodies. The immunoprecipitates were eluted and reverse cross-linked overnight at 65°C. DNA fragments were purified using the Cycle Pure kit (Omega Bio-Tek, Inc., Norcross, GA), and qPCR was performed for quantification.

RESULTS

Satellite cell-specific NICD^{OE} promotes the self-renewal of myogenic progenitors. To investigate the role of Notch signaling in postnatal satellite cells, we established *Pax7-Cre^{ER}/ROSA-N1ICD* (called Pax7-NICD^{OE}) mice (Fig. 1A). In this model, Cre-dependent expression of N1ICD and nuclear GFP is driven by the ubiquitously expressed endogenous Rosa26 promoter. Upon activation of Cre^{ER} by Tamoxifen (TAM), NICD is specifically expressed in Pax7-expressing satellite cells. The expression of GFP in the nucleus serves as a marker to identify which cells have NICD^{OE}. To examine how Notch signaling regulates the cell fate dynamics of satellite cells, we dissociated single EDL myofibers and cultured them in suspension to activate satellite cells. Suspended culture of satellite cells while still attached to host myofibers provides an excellent *in vitro* model for analyzing cell fate segregation among self-renewal, proliferation, and differentiation based on Pax7 and MyoD expression. Specifically, activated satellite cells (called myoblasts) undergoing self-renewal, proliferation, and differentiation can be distinguished as Pax7$^+$ MyoD$^-$, Pax7$^+$ MyoD$^+$, and Pax7$^-$ MyoD$^+$, respectively (16, 32, 55).

EDL myofibers from control and Pax7-NICD^{OE} mice pretreated with TAM were cultured for 72 h and labeled with Pax7, MyoD, and GFP (Fig. 1A). Whereas the majority of the myoblasts on the control EDL myofibers coexpressed Pax7 and MyoD (Fig. 1B, left panels), the NICD^{OE} myoblasts (labeled with GFP) exhibited reduced MyoD expression (Fig. 1B, right panels). This observation is consistent with previous reports that Notch signaling inhibits myogenic differentiation. However, it is unclear whether the myoblasts blocked from differentiation are in the proliferation or self-renewal state. To address this, we quantified the percentage of self-renewing (Pax7$^+$ MyoD$^-$), proliferating (Pax7$^+$ MyoD$^+$), and differentiating cells (Pax7$^-$ MyoD$^+$). Strikingly, the proportions of self-renewing cells doubled (Fig. 1C), while proliferating cells were reduced (Fig. 1D), on the NICD^{OE} myofibers.

As nuclear GFP expression distinguishes whether a cell expresses the constitutive activated N1ICD (GFP$^+$) or not (GFP$^-$), we further analyzed the GFP$^+$ and GFP$^-$ cell populations on cultured Pax7-NICD^{OE} myofibers (Fig. 1B, right panels). Consistent with our earlier finding, over 90% of the GFP$^+$ cells were self-renewing, while only 10% of the GFP$^-$ cells were self-renewing (Fig. 1E, left). On the other hand, less than 10% of the GFP$^+$ cells proliferated, while nearly 80% of the GFP$^-$ cells proliferated (Fig. 1E, right). Overall, the average number of myoblasts within each colony of cells growing on the Pax7-NICD^{OE} myofibers was reduced compared to the control myofibers at 72 h (Fig. 1F). Using the same culture paradigm, *de novo* activation of Notch by using adenovirus-mediated Cre transduction further confirmed the above observations (data not shown). Together, these results provide compelling evidence that NICD^{OE} promotes self-renewal of activated satellite cells while inhibiting their proliferation.

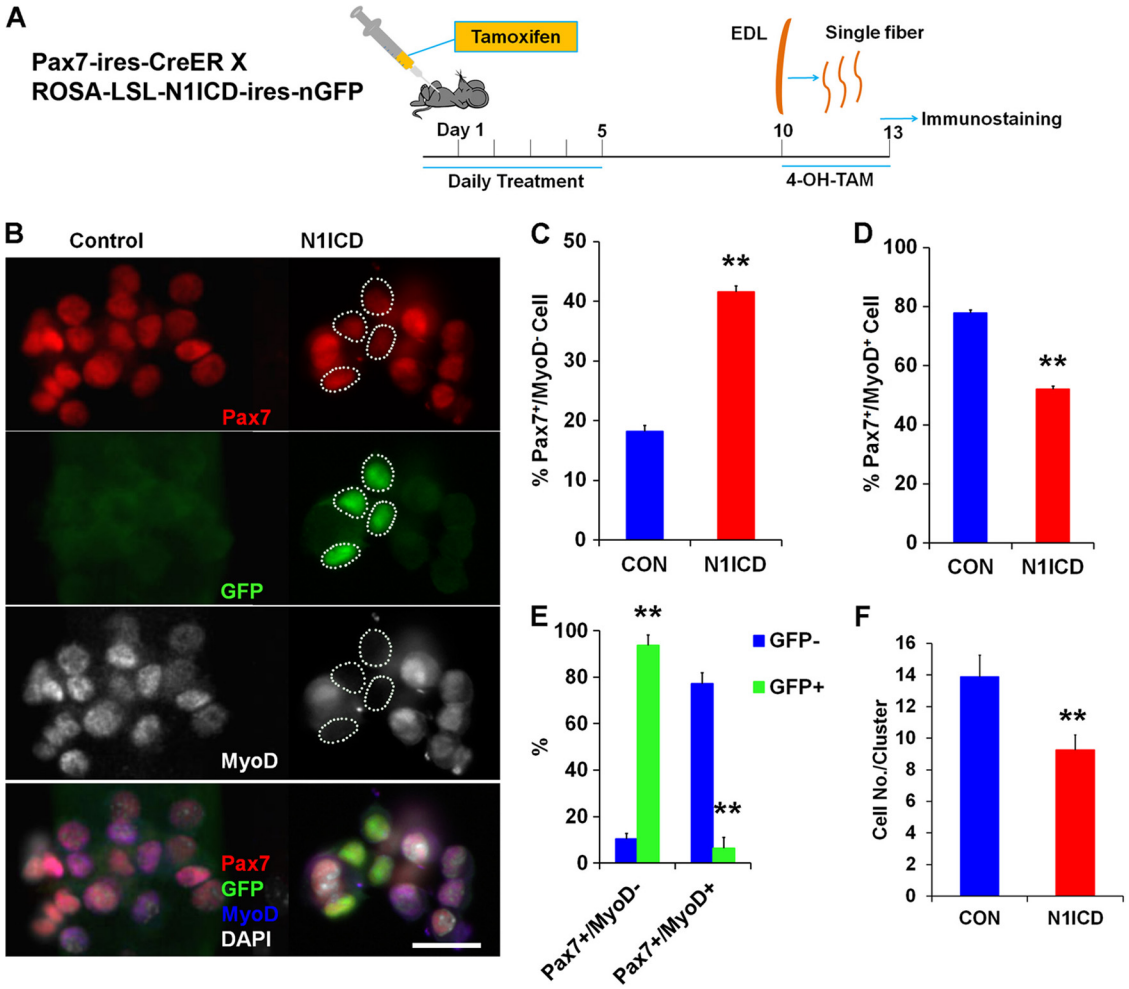

FIG 1 Overexpression of N1ICD promotes the self-renewal of satellite cells. (A) Experimental design. Results are based on Pax7-Cre^{ER}/Rosa-N1ICD mice, in which N1ICD^{OE} is induced by 4-OH-TAM and N1ICD^{OE} myoblasts coexpress nEGFP (nuclear localized GFP). Satellite cells undergo activation, proliferation, self-renewal, and differentiation while attached on their host myofibers. (B) Myoblast clusters on cultured single fibers were labeled with antibodies against Pax7, MyoD, and GFP. Nuclei were counterstained with 4′,6-diamidino-2-phenylindole (DAPI). Note that GFP marks the N1ICD^{OE} myoblasts. Dotted circles indicate the lack of MyoD staining in GFP$^+$ cells. Bar, 20 μm. (C and D) Percentage of self-renewing (Pax7$^+$ MyoD$^-$) and proliferating (Pax7$^+$ MyoD$^+$) myobalsts in control and N1ICD^{OE} myoblast colonies (calculated from 28 cultured colonies in each group). (E) Percentage of self-renewing Pax7$^+$ MyoD$^-$ and proliferating Pax7$^+$ MyoD$^+$ myobalsts for GFP$^-$ (~30%) and GFP$^+$ (~70%) subpopulations among N1ICD^{OE} myoblast clusters (n = 28). (F) Number of myoblasts per cluster in control and N1ICD^{OE} myofiber cultures (n = 28).

NICD^{OE} inhibits the proliferation of primary myoblasts. That constitutive Notch activation inhibits myoblast proliferation was totally unexpected, as previous studies indicated that Notch signaling promoted proliferation. To confirm this novel observation, we compared the growth curves and BrdU incorporation and Ki67 expression levels of control and NICD^{OE} primary myoblasts. *ROSA-N1ICD* myoblasts were transfected with a *Cre* plasmid to induce NICD^{OE}, which resulted in a 3.5-fold increase in *N1ICD* transcripts and a 6-fold increase in Notch target *Hey1* gene expression (Fig. 2A). Such a moderate upregulation of Notch signaling may represent a more "physiological" condition. Next, we compared the growth of Pax7-Cre^{ER}/ROSA-N1ICD myoblasts treated with vehicle control or 0.4 uM 4-hydroxy-TAM, which activates overexpression of NICD. Strikingly, the NICD^{OE} myoblasts exhibited much-reduced growth rates at all time points examined (Fig. 2B). These results demonstrated that NICD^{OE} inhibits the growth of myoblasts in culture.

We next incubated myoblasts with BrdU for 24 h and quantified the percentage of S-phase cells, based on BrdU incorporation and using a *Cre* plasmid to activate NICD (Fig. 2C). As *Cre* transfection induces coexpression of GFP and N1ICD in *ROSA-N1ICD* cells, GFP expression distinguishes whether a cell expresses the constitutively activated N1ICD (GFP$^+$) or not (GFP$^-$). Importantly, NICD^{OE} (GFP$^+$) cells were predominately BrdU$^-$ (Fig. 2C, arrows). Conversely, BrdU$^+$ cells were almost all GFP$^-$ (see Fig. 2C [asterisks], below). Overall, the percentage of BrdU$^+$ cells was significantly reduced in *Cre*-transfected cells compared to control empty plasmid-transfected cells (Fig. 2C, graph). This mutually exclusive expression pattern of GFP (NICD^{OE}) and BrdU incorporation (DNA synthesis) indicated that NICD^{OE} inhibits S-phase entry of myoblasts.

In addition, we analyzed the expression of the cell proliferation marker Ki67 in *ROSA-N1ICD* myoblasts transfected with *Cre* or empty plasmids. Consistent with the BrdU incorpora-

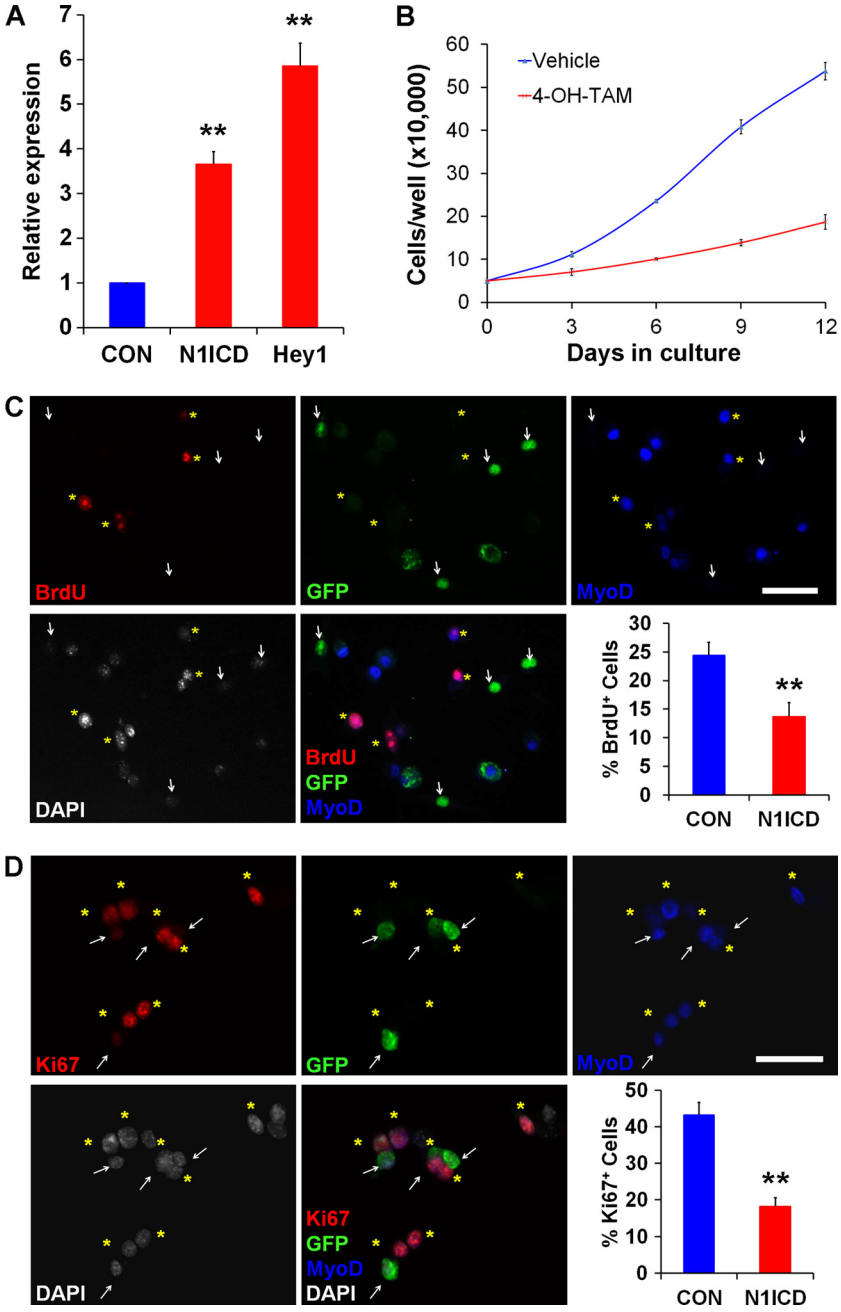

FIG 2 Overexpression of N1ICD inhibits myoblast proliferation. Results are based on Rosa-N1ICD myoblasts electrotransfected with pGK-Cre or empty plasmids. Cre^+ myoblasts ($N1ICD^{OE}$) are marked by nGFP, while Cre^- cells (control) don't exhibit GFP staining. (A) Expression levels of *N1ICD* and *Hey1* upon electroporation of pGK-Cre in Rosa-N1ICD myoblasts ($n = 3$). Results in panels C and D, below, are based on this $N1ICD^{OE}$ strategy. (B) Growth rates of $Pax7\text{-}Cre^{ER}$/Rosa-N1ICD myoblasts treated with vehicle (control) or 4-OH-TAM (0.4 μM), which activates N1ICD in Pax7-expressing myoblasts ($n = 3$). (C) BrdU incorporation by GFP^+ and GFP^- Rosa-N1ICD myoblasts transfected with pGK-Cre. Arrows show that GFP^+ myoblasts failed to incorporate BrdU and lacked the expression of MyoD. Asterisks indicate GFP^- myoblasts that incorporated BrdU and expressed MyoD. The bar graph shows the percentage of $BrdU^+$ cells in Rosa-N1ICD myoblasts transfected with empty (CON) or pGK-Cre (N1ICD) plasmids ($n = 3$). Bar, 40 μm. (D) Proliferating cell marker Ki67 expression in GFP^+ and GFP^- Rosa-N1ICD myoblasts transfected with pGK-Cre. Arrows show that GFP^+ myoblasts were $Ki67^-$ and mostly $MyoD^-$. Asterisks indicate GFP^- myoblasts that expressed Ki67 and MyoD normally. The bar graph shows the percentage of $Ki67^+$ cells in Rosa-N1ICD myoblasts transfected with empty (CON) or pGK-Cre (N1ICD) plasmids ($n = 3$). Bar, 40 μm.

tion results, GFP expression, which marks $NICD^{OE}$, and Ki67 expression were mutually exclusive (Fig. 2D). The overall percentage of $Ki67^+$ cells in *Cre*-transfected culture was less than half that in the control group (Fig. 2D, graph). Together, our growth curve, BrdU uptake, and Ki67 expression analyses provided convincing evidence for an inhibitory role of constitutively activated Notch in the proliferation of satellite cell-derived primary myoblasts.

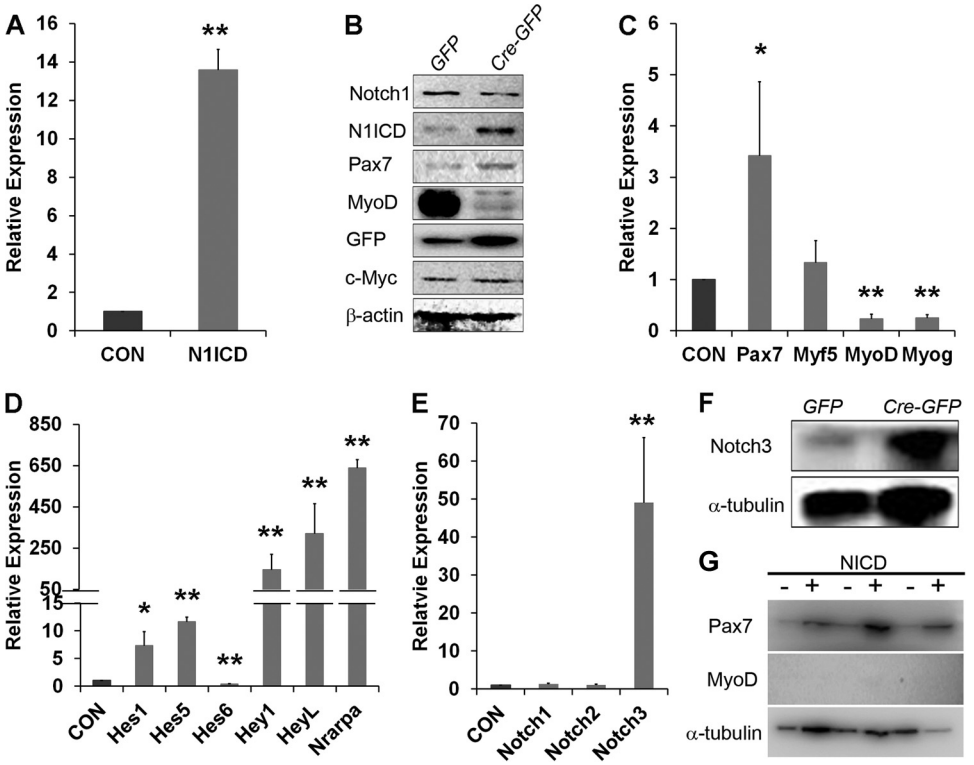

FIG 3 N1ICD^{OE} upregulates Pax7 and elicits coordinated changes in the expression of Notch-related genes. (A) Relative levels of *N1ICD* expression in myoblasts treated with adenovirus-GFP (normalized to 1) or adenovirus-Cre ($n = 3$). (B) Western blots showing changes in N1ICD and myogenic proteins in Rosa-N1ICD myoblasts treated with adenovirus-GFP or adenovirus-Cre. (C) Relative expression levels of myogenic genes *Pax7*, *Myf5*, *MyoD*, and *Myogenin* in myoblasts treated with adenovirus-GFP (normalized to 1) or adenovirus-Cre ($n = 3$). (D) Relative expression levels of Notch target genes *Hes1*, *Hes5*, *Hes6*, *Hey1*, *HeyL*, and *Nrarpa* in Rosa-N1ICD myoblasts treated with adenovirus-GFP (normalized to 1) or adenovirus-Cre ($n = 3$). (E) Relative expression levels of *Notch* receptor genes in myoblasts treated with adenovirus-GFP (normalized to 1) or adenovirus-Cre ($n = 3$). (F) Representative Western blot confirming the increased protein level of the Notch3 receptor in Rosa-N1ICD myoblasts treated with adenovirus-Cre. (G) NICD^{OE} upregulates Pax7 independently of MyoD. Primary myoblasts were isolated from MyoD$^{-/-}$ mice and transfected with a RAMIC plasmid to overexpress N1ICD (+). Control (−) myoblasts were transfected with an empty plasmid.

NICD^{OE} upregulates Pax7 and elicits coordinated changes in target gene expression. To identify potential target genes mediating the effect of Notch signaling in satellite cell self-renewal, we analyzed the expression of a number of genes involved in the Notch signaling pathway as well as Pax7, which is known to be critical for satellite cell self-renewal in control and NICD^{OE} myoblasts. NICD^{OE} was induced by adenovirus-mediated *Cre* transduction into ROSA-N1ICD myoblasts. NICD^{OE} resulted in a 14-fold increase in *N1ICD* transcript levels compared to the control treatment, in which the same myoblasts were transduced with adenovirus-GFP (Fig. 3A). Western blot analysis confirmed the increased N1ICD and GFP expression in *Cre*-transduced cells, but the endogenous Notch1 receptor expression remained unchanged (Fig. 3B). As expected, MyoD protein was dramatically reduced by NICD^{OE}, validating the effectiveness of the treatment. What interested us was that Pax7 protein was also increased in the NICD^{OE} cells (Fig. 3B). To confirm this result, we examined the mRNA by qPCR. Again, *Pax7* mRNA was increased by 3.5-fold, whereas *MyoD* and *Myogenin* were both decreased by 3- to 4-fold in NICD^{OE} cells (Fig. 3C). As MyoD has been reported to inhibit Pax7, we further investigated if Pax7 upregulation is a secondary effect of MyoD inhibition by Notch activation. We overexpressed N1ICD in MyoD$^{-/-}$ myoblasts and observed robust upregulation of Pax7 (Fig. 3G). Thus, Notch activation upregulated Pax7 in the absence of MyoD. Our results indicate that NICD^{OE} upregulates Pax7 at both mRNA and protein levels independent of MyoD inhibition, resulting in enhanced self-renewal of satellite cells.

To provide insights into how NICD^{OE} upregulates Pax7, we examined Notch target genes that are coregulated with Pax7. Interestingly, *Nrarp* and Hey family genes *Hey1* and *HeyL* were most robustly upregulated, with 140- to 640-fold increases induced by NICD^{OE} (Fig. 3D). The Hes family genes were modestly upregulated, with 7-fold and 12-fold increases in the expression levels of *Hes1* and *Hes5*, respectively (Fig. 3D). In contrast, *Hes6* expression was reduced by 70% in NICD^{OE} cells (Fig. 3D). Moreover, we examined the expression of Notch receptors in order to understand if there was a compensatory reduction of endogenous Notch receptors. Whereas *Notch1* and *Notch2* expression levels were not affected, *Notch3* expression was unexpectedly increased by 50-fold in NICD^{OE} cells (Fig. 3E). Consistently, Notch3 protein was also robustly upregulated by NICD^{OE} (Fig. 3F). Therefore, NICD^{OE} results in increased Pax7 expression and coordinated alterations in the expression of Notch receptor and target genes in primary myoblasts.

Notch signaling regulates satellite cell self-renewal, proliferation, and differentiation through distinct targets. As *Pax7* upregulation is correlated with corresponding increases with *Hes*, *Hey*, and *Nrarp* genes, we asked if *Pax7* expression is regulated by these canonical Notch targets. To address this, we individually overexpressed *Hes*, *Hey*, and *Nrarp* genes in primary myoblasts

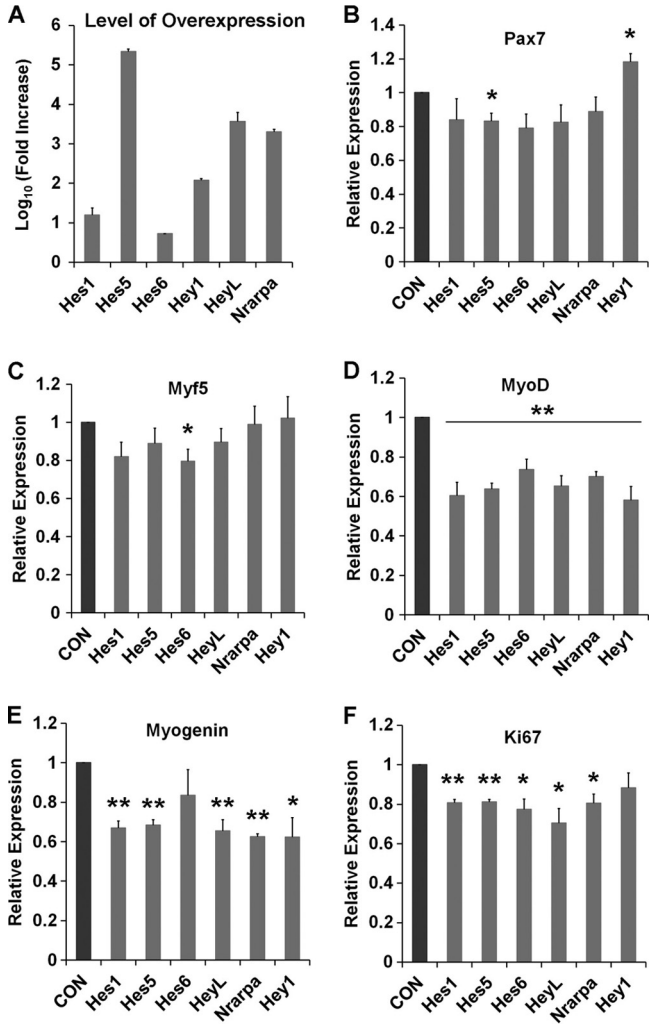

FIG 4 Canonical Notch target genes mimic the effects of N1ICD^{OE} in the suppression of *MyoD*, *Myogenin*, and *Ki67* but fail to upregulate Pax7. (A) Fold increases (on a log scale) of various Notch target gene expression levels upon transfection of corresponding plasmids to overexpress *Hes1*, *Hes5*, *Hes6*, *Hey1*, *HeyL*, and *Nrarpa* ($n = 5$). (B to F) Fold changes of *Pax7* (B), *Myf5* (C), *MyoD* (D), *Myogenin* (E), and *Ki67* (F) gene expression in response to *Hes1*, *Hes5*, *Hes6*, *Hey1*, *HeyL*, and *Nrarpa* gene overexpression. Fold changes are relative to control myoblasts transfected with empty plasmids (normalized to 1) ($n = 3$).

(Fig. 4A), which led to 8- to 1,000-fold increases in their expression (except for *Hes5*, whose expression was increased by 100,000-fold due to extremely low *Hes5* expression in control cells). To our surprise, none of these overexpressed genes was able to mimic the effect of NICD^{OE} on *Pax7* expression (Fig. 4B). Although overexpression of *Hey1* resulted in a 20% increase in *Pax7*, this increase was not near the 3-fold increase induced by NICD^{OE}. Overexpression of other genes either reduced or had no effect on *Pax7* expression (Fig. 4B). Consistent with the NICD^{OE} results (Fig. 3C), *Myf5* expression was largely unaffected by the Notch target genes (Fig. 4C). In contrast, individual overexpression of all the Notch target genes resulted in roughly 40% suppression of *MyoD* (Fig. 4D), and all genes except for Hes6 suppressed *Myogenin* gene expression (Fig. 4E). Intriguingly, individual overexpression of Notch target genes also led to 20 to 30% reductions in *Ki67* expression (Fig. 4F). These results are consistent with our previous observation that NICD^{OE} inhibits myoblast proliferation. Collectively, these overexpression experiments suggest that Notch signaling regulates satellite cell fate choice through distinct mediators: while Notch suppresses proliferation and differentiation through canonical Hes, Hey, and Nrarp proteins, Notch regulates self-renewal (Pax7) independent of these canonical targets.

N1ICD directly regulates Pax7 expression through RBP-Jκ. As canonical Notch targets Hes, Hey, and Nrarpa had no effect on *Pax7* expression, we hypothesized that N1ICD directly regulates *Pax7*. Analysis of the *Pax7* upstream genomic sequence identified two RBP-Jκ consensus binding sites (GTGGGAA) (Fig. 5A). To investigate if they are associated with RBP-Jκ, we performed a chromatin immunoprecipitation (ChIP) assay. Indeed, both binding sites were enriched by more than 5-fold in the ChIP assay with RBP-Jκ antibody (Fig. 5B and C), suggesting that RBP-Jκ occupies these sequences in the *Pax7* promoter region. Importantly, ChIP analysis using N1ICD antibody also led to 2- to 3-fold enrichment of these binding sites (Fig. 5B and C), indicating that N1ICD is also associated with the RBP-Jκ consensus binding sites in the *Pax7* gene upstream region. In contrast, both Pax7 and RBP-Jκ failed to enrich DNA fragments 200 bp away from the consensus RBP-Jκ binding sites (Fig. 5D and E), confirming the specificity of N1ICD and RBP-Jκ binding. As the N1ICD enrichment of target DNA is lower than that by RBP-Jκ, we predicted that the association between N1ICD and *Pax7* promoter regions is mediated by RBP-Jκ. Consistent with this notion, lentivirus-mediated shRNA knockdown of *RBP-Jκ* abolished the enrichment of the target DNA sequences by both N1ICD and RBP-Jκ antibodies (Fig. 5F and G) and resulted in decreased Pax7 expression (Fig. 5H). Together, these results provide strong biochemical and functional evidence that N1ICD directly regulates Pax7 gene expression through RBP-Jκ.

Satellite cell-specific NICD^{OE} impairs the regeneration of postnatal skeletal muscles. Previous reports showed that activation of Notch signaling restores the regenerative deficiencies of aged muscles (8). However, it has not been shown if muscle satellite cell-specific Notch activation is responsible for such improvements in muscle regeneration. To address this question, we examined the regenerative response of acutely injured TA muscles of Pax7-NICD^{OE} and wild-type mice. Both types of mice were treated with TAM for 5 days, followed by a 5-day waiting period to allow for Cre-mediated activation of *N1ICD*, and then treated with CTX to degenerate the TA muscles. The regenerative efficiency was evaluated at 7 and 21 days postinjection (dpi) of CTX (Fig. 6A). NICD^{OE} in quiescent satellite cells did not alter the satellite cell number in the resting (noninjured) EDL muscles (Fig. 6B), suggesting that muscle regeneration was mediated by equal numbers of satellite cells prior to CTX-induced injury. At 7 dpi, the damaged muscles were fully replaced by newly regenerated myofibers characterized by centrally localized myonuclei in the control mice (Fig. 6C). However, the injured Pax7-NICD^{OE} muscles were poorly repaired, with increased interstitial space and adipose infiltration (Fig. 6D). At 21 dpi, the regenerated myofibers became significantly larger and the muscle structure was restored in the control mice (Fig. 6E and G). By sharp contrast, the regenerated myofibers remained small, and large interstitial spaces were evident in the NICD^{OE} mice (Fig. 6F and G). At 7 dpi, the number of regenerating myofibers per microscopic field (~0.15 mm^2) was reduced by 50% in the Pax7-NICD^{OE} compared to the control

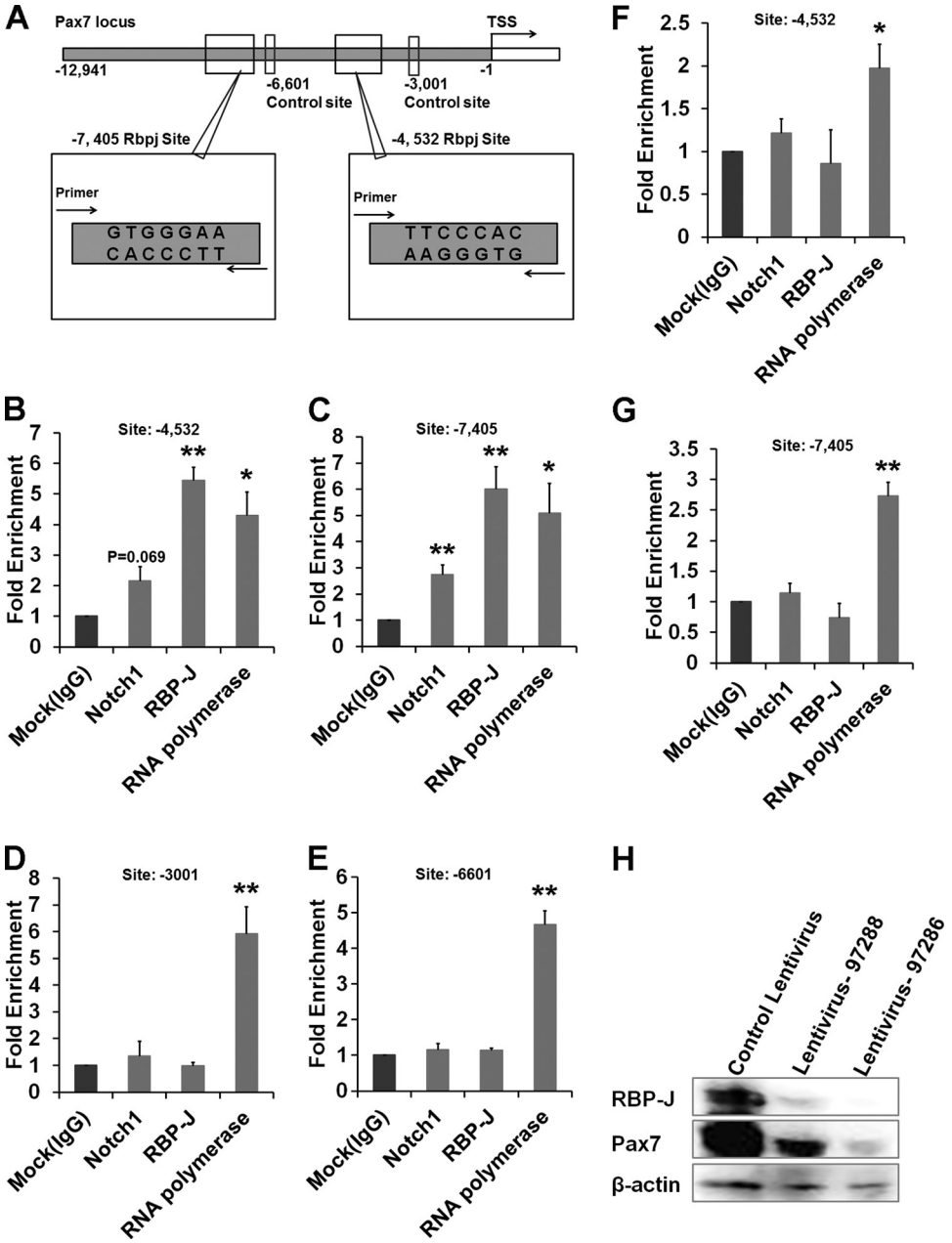

FIG 5 N1ICD directly regulates Pax7 through consensus RBP-Jκ binding. Results were based on ChIP analysis of enrichment of DNA fragments surrounding evolutionally conserved RBP-Jκ GTGGGAA-binding motifs upstream of the *Pax7* allele. (A) DNA sequence analysis identified conserved RBP-Jκ-binding sites upstream of the transcriptional start site of *Pax7*. Nonbinding sites were selected as negative controls for DNA enrichment analysis. (B and C) ChIP assay combined with quantitative PCR results, showing enrichment of two RBP-Jκ-binding sites at nucleotide positions −4532 and −7405, based on both anti-Notch1 and anti-RBP-Jκ antibodies ($n = 3$). RNA polymerase antibody was used as a positive control, and mock IgG was used as a negative control for nonspecific binding. (D and E) Two nonbinding sites (−3001 and −6601) were selected for ChIP-PCR analysis to show the lack of enrichment by anti-Notch1 or anti-RBP-Jκ but strong enrichment by RNA polymerase antibody ($n = 3$). (F and G) ChIP-PCR results after shRNA knockdown of RBP-Jκ. Enrichments by Notch1 and RBP-Jκ were both abolished at the −4532- and −7405-binding sites, while the enrichment by RNA polymerase was not affected by RBP-Jκ knockdown ($n = 3$). (H) shRNA-mediated knockdown of RBP-Jκ inhibits Pax7 expression in primary myoblasts. Two lentiviral knockdown vectors (97288 and 97286) together with an empty lentiviral vector (control) were used.

muscles (Fig. 6H). Interestingly, due to their extreme small size, the number of regenerating myofibers per unit area was increased by 50% in the $NICD^{OE}$ compared to the control mice at 21 dpi (Fig. 6G and H). In contrast to the markedly reduced muscle regeneration, the number of $Pax7^{+}$ progenitors was strikingly increased in the regenerating Pax7-$NICD^{OE}$ muscle cells compared to the control muscles at both 7 and 21 dpi (Fig. 6K). Finally, analysis of phospho-histone 3 (PH3) expression (Fig. 6L and M) indicated that $NICD^{OE}$ reduced satellite cell proliferation (Fig. 6N). Thus, constitutive activation of Notch in postnatal satellite cells reduced their proliferation and differentiation but enhanced satellite cell self-renewal, leading to impaired muscle regeneration *in vivo*.

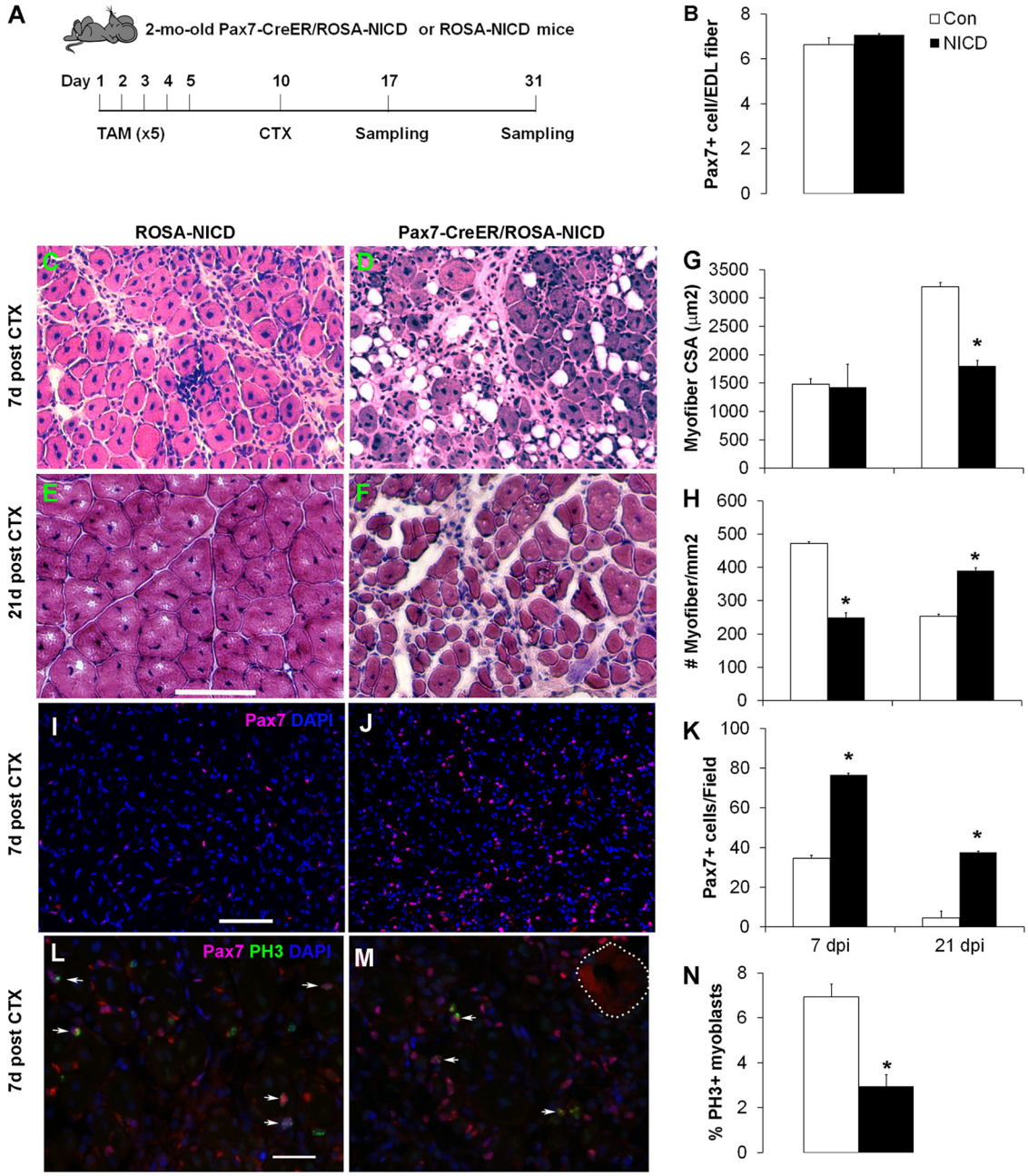

FIG 6 Satellite cell-specific N1ICD^{OE} leads to defective muscle regeneration. (A) Experimental design. Two-month-old littermate control (ROSA-N1ICD) and N1ICD^{OE} (Pax7-Cre^{ER}/Rosa-N1ICD) mice were injected intraperitoneally with 5 doses of Tamoxifen. TA muscles are subsequently injected with CTX to induce regeneration, and samples were collected at 7 and 21 dpi of CTX. (B) N1ICD^{OE} did not affect the number of quiescent Pax7^{+} satellite cells per EDL myofiber in noninjured (resting) muscles ($n = 3$ pairs of mice, >20 fibers per EDL muscle analyzed). (C and D) Representative H&E staining of regenerating TA muscles at 7 dpi in control (C) and N1ICD^{OE} (D) mice. Red cells with central nuclei represent regenerating myofibers, and white round cells are adipocytes. (E and F) The same experiment as shown in panels C and D, but at 21 dpi. Bar, 100 μm (C to F). (G) Number of regenerated myofibers/mm^2 in control and N1ICD^{OE} TA muscles at 7 dpi ($n = 4$) and 21 dpi ($n = 3$ pairs of mice). (H) Average CSA of regenerated fibers in control and N1ICD^{OE} TA muscles at 7 dpi ($n = 4$) and 21 dpi ($n = 3$ pairs of mice). (I and J) Representative Pax7 immunostaining images of regenerating TA muscles in the control (I) and N1ICD^{OE} (J) mice at 7 dpi. Bar, 50 μm. (K) Average number of Pax7^{+} cells per field (~0.15 mm^2) in control and N1ICD^{OE} TA muscles at 7 dpi ($n = 4$) and 21 dpi ($n = 3$ pairs of mice). (L and M) Representative images of phospho-histone 3 (PH3) and Pax7 double labeling of regenerating TA muscles in control (L) and N1ICD^{OE} (M) mice at 7 dpi. The dotted line in panel M indicates a degenerated myofiber. Bar, 20 μm. (N) Percentage of PH3^{+} metaphase satellite cells in control and N1ICD^{OE} regenerating TA muscles at 7 dpi ($n = 3$ pairs of mice).

DISCUSSION

Postnatal muscle growth, maintenance, and regeneration are mediated by muscle-specific stem cells (satellite cells) that are capable of self-renewal and myogenic differentiation. Upon activation, satellite cell progenies adopt divergent cell fates: while some remain in the cell cycle and proliferate, others withdraw from the cell cycle and self-renew or differentiate (55). To investigate the potential role of Notch signaling in the cell fate specification of

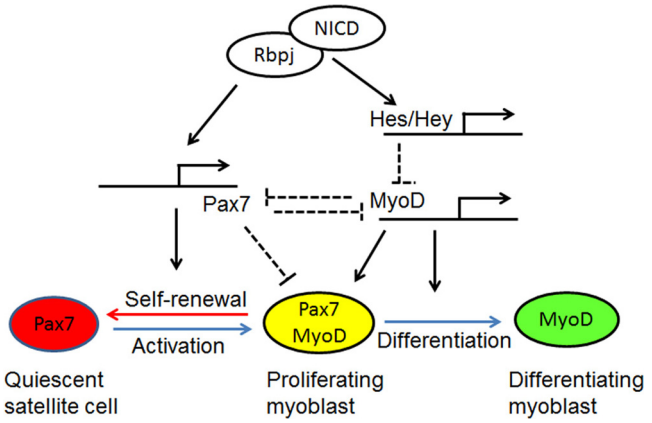

FIG 7 Model for Notch's regulation of stem cell fate in muscle. Quiescent satellite cells (stem cells) express high levels of Pax7. The activated satellite cells (myoblast) coexpress Pax7 and MyoD and proliferate. The proliferating myoblast can either downregulate Pax7 to differentiate or downregulate MyoD to self-renew. Activated Notch (NICD) binds to RBP-Jκ to form a transcriptional activation complex that upregulates the transcription of Pax7 as well as canonical Notch targets (Hes and Hey family genes). Hes/Hey proteins inhibit MyoD gene transcription. Therefore, Notch activation upregulates Pax7 to promote satellite cell self-renewal, while inhibiting MyoD to block myogenic differentiation. Pax7 upregulation and MyoD downregulation may together lead to cell cycle withdrawal. The reciprocal inhibitory action between Pax7 and MyoD further amplifies the effect of Notch signaling.

muscle stem cells, we specifically activated Notch1 in postnatal satellite cells and revealed several novel roles of Notch signaling. We found that NICD^{OE} inhibited myoblast proliferation. We also discovered a role of Notch signaling in the self-renewal of satellite cells independent of inhibition of myogenic differentiation (Fig. 7). Furthermore, we elucidated the molecular mechanisms through which Notch regulates *Pax7*.

Although *in vivo* analysis of Notch gain- and loss-of-function mutants demonstrated an important role of Notch signaling in myogenic lineage development and postnatal muscle regeneration, it has been unknown if Notch signaling regulates self-renewal and differentiation independently or if Notch only blocks differentiation, which subsequently affects the balance between self-renewal and differentiation (Fig. 7). Our analysis of satellite cell fate choice on cultured myofibers supports a conclusion that Notch^{OE} enhances the self-renewal of activated satellite cells through upregulation of Pax7. Previous studies established that Notch activation robustly inhibits the expression of MyoD and Myogenin, which have been shown to be able to repress the expression of Pax7 (34). These results led to the speculation that Notch-induced Pax7 upregulation is a secondary consequence due to MyoD and Myogenin inhibition (49). Our studies clearly demonstrated that whereas *Hes1*, *Hes5*, *Hey1*, *HeyL*, and *Nrarp* overexpression all suppressed the expression of *MyoD* and *Myogenin*, they had little effect on *Pax7*. Thus, NICD^{OE}-induced Pax7 upregulation is not mediated by the canonical Notch targets and is thus independent of MyoD/Myogenin suppression. The relatively modest inhibition of *MyoD*/*Myogenin* by individual canonical Notch targets compared to the level of inhibition by NICD^{OE} could be due to several possibilities. First, NICD^{OE} alters the expression of a repertoire of target genes whose coordinated changes define the final level of *MyoD*. Thus, individually manipulating these genes cannot fully recapitulate the effect of NICD^{OE}. Second, overexpression of *Hes/Hey* target genes had no effect on Pax7 expression, while NICD^{OE} upregulated Pax7, which may further inhibit MyoD expression. It will be interesting to investigate if Notch-induced Pax7 upregulation contributes to the downregulation of MyoD, as shown in other studies (32–34).

Our current results, indicating that Notch upregulates Pax7 and promotes satellite cell self-renewal, are consistent with several recent studies. Specifically, two recent studies indicated that Notch signaling is required for maintaining the quiescence of satellite cells (2, 28). This conclusion is consistent with our results that Notch activation promotes self-renewal of activated satellite cells. It has also been shown that pharmacological inhibition of Notch signaling decreased self-renewing progeny in satellite cell cultures and Dll1-induced Notch activation increased Pax7 expression (23, 49). However, how Notch regulates Pax7 at the molecular level is unknown. Using ChIP analysis we demonstrated that N1ICD and RBP-Jκ are both associated with the Pax7 promoter region. Importantly, lentivirus-mediated shRNA knockdown of RBP-Jκ not only abolished the physical association between N1ICD and the Pax7 promoter but also functionally inhibited *Pax7* gene expression. These results provide strong evidence that N1ICD directly regulates Pax7 expression through RBP-Jκ, but this is independent of inhibition of MyoD and Myogenin, which is mediated by Hes and Hey family proteins.

Our growth curve analysis, BrdU incorporation, Ki67 assays, and gene expression analysis all suggest that Notch activation inhibits the proliferation of primary myoblasts. These results were unexpected, although they are in line with a recent study showing that *Notch3* mutation enhanced the proliferation of primary myoblasts (19). Indeed, we observed elevated expression of *Notch3* in NICD^{OE} myoblasts, consistent with previous results showing that Notch3 was increased by N1ICD and downregulated by the γ-secretase inhibitor in T6E cells (53). In addition, our observation is consistent with recent studies demonstrating that compound mutation of Notch targets *Hey1* and *HeyL*, or mutation of *Rbpj*, leads to loss of quiescence in satellite cells and spontaneous entry into the cell cycle or differentiation (2, 14, 28). Moreover, upregulation of Pax7 itself may act as a regulator to withdraw satellite cells from the cell cycle (32). In contrast, several previous studies indicate that Notch activation promotes myoblast proliferation. Specifically, retroviral transduction of constitutively activated Notch1 into primary myoblasts increased their proliferation, whereas transfection of Numb, a Notch inhibitor, inhibited myoblast proliferation (10). At the molecular level, activation of Notch signaling blocks TGF-β-induced upregulation of cyclin-dependent kinase (CDK) inhibitors p21, p15, p16, and p27 (6). Interestingly, several studies have demonstrated that Notch inhibits proliferation through upregulation of p21 in other systems (45). Thus, whether Notch activation stimulates or inhibits proliferation is highly cell context dependent. The contradictory effects of Notch activation on myoblast proliferation observed by different groups may also be due to culture conditions, as growth factors drastically influence the outcome of Notch activation in hematopoietic progenitor cells (52). As these studies were all performed *in vitro*, it is imperative to clarify how Notch activation affects satellite cell proliferation *in vivo*.

The perinatal lethality caused by constitutive activation (Bi P, et al, unpublished data) or inactivation of Notch signaling in myogenic cell lineages during embryonic myogenesis precludes analysis of postnatal satellite cells and muscle regeneration *in vivo*. To

circumvent the lethality problem, we used Tamoxifen-inducible Pax7-Cre^{ER} mice to drive NICD^{OE} in postnatal satellite cells and examined muscle regeneration *in vivo*. We found that satellite cell-specific NICD^{OE} inhibited muscle regeneration, accompanied by increased Pax7^{+} cells, due to enhanced self-renewal and reduced differentiation of activated satellite cells. This observation is consistent with the developmental phenotypes associated with Notch mutation, which resulted in the ablation of satellite cells (44, 50). However, these results are in contrast to previous observations that Notch activation improves muscle regeneration in old mice (8). This discrepancy may be caused by several mechanisms. First, Conboy et al. injected recombinant proteins (Jagged1-Fc and Notch1 antibody) to injury sites to inhibit and activate Notch signaling, respectively (8). Therefore, the inhibition and activation of Notch signaling are transient (depending on protein stability), focal (at the injection site), and nonspecific (any cells near the injection site can be targeted). In contrast, our genetic activation approach specifically activates Notch in Pax7-expressing cells (satellite cells in the muscle) and results in widespread expression (no physical boundaries). Second, previous results were based on aged mice (23 to 24 months old), but our current results were based on experiments in young mice (2 to 3 months old). However, given the well-established inhibitory role of Notch in myogenic differentiation, we predict that constitutive Notch activation will similarly inhibit the regeneration of old muscles, while transiently activating Notch may facilitate the regeneration. Indeed, the age-associated decline in muscle injury repair is reported to be largely attributed to decreased activation of satellite cells by Notch signaling, and Wnt-mediated inhibition of Notch signaling is necessary for myogenic differentiation (5, 9, 43). Third, the amplitude of Notch activation may have been different in these different studies. Together, Notch signaling must be dynamically regulated at different stages (activation, proliferation, and differentiation) in order for damaged muscle to regenerate properly.

ACKNOWLEDGMENTS

Contributions of the authors were the following: Yefei Wen, conception and design of experiments, collection and assembly of data, data analysis and interpretation, manuscript writing, and final approval of the manuscript; Pengpeng Bi, collection and assembly of data, paper revision, and final approval of the manuscript; Weiyi Liu, collection and assembly of data and final approval of the manuscript; Atsushi Asakura, provision of MyoD$^{-/-}$ primary myoblasts and final approval of the manuscript; Charles Keller, provision of Pax7-Cre^{ER} mouse and final approval of the manuscript; Shihuan Kuang, conception and design of experiments, financial support, administrative support, provision of study materials, data analysis and interpretation, manuscript writing, and final approval of the manuscript.

We thank Yong-Xu Wang (University of Massachusetts School of Medicine) for the adeno-Cre virus, Philip Soriano (MSSM) for Myf5-Cre mice, and Kazuki Kuroda for the NICD^{OE} plasmid. We appreciate the advice of Michael Rudnicki and the technical assistance of Jian Luo.

The project was supported by funding from the MDA, NIH, and USDA to S.K.

We declare no conflicts of interest.

REFERENCES

1. **Acharyya S, et al.** 2010. TNF inhibits Notch-1 in skeletal muscle cells by Ezh2 and DNA methylation mediated repression: implications in duchenne muscular dystrophy. PLoS One **5**:e12479. doi:10.1371/journal.pone.0012479.
2. **Bjornson CR, et al.** 2011. Notch signaling is necessary to maintain quiescence in adult muscle stem cells. Stem Cells **30**:232–242.
3. **Brack AS, Conboy IM, Conboy MJ, Shen J, Rando TA.** 2008. A temporal switch from notch to Wnt signaling in muscle stem cells is necessary for normal adult myogenesis. Cell Stem Cell **2**:50–59.
4. **Buas MF, Kabak S, Kadesch T.** 2010. The Notch effector Hey1 associates with myogenic target genes to repress myogenesis. J. Biol. Chem. **285**:1249–1258.
5. **Carlson BM.** 2003. Muscle regeneration in amphibians and mammals: passing the torch. Dev. Dyn. **226**:167–181.
6. **Carlson ME, Hsu M, Conboy IM.** 2008. Imbalance between pSmad3 and Notch induces CDK inhibitors in old muscle stem cells. Nature **454**:528–532.
7. **Charge SB, Brack AS, Hughes SM.** 2002. Aging-related satellite cell differentiation defect occurs prematurely after Ski-induced muscle hypertrophy. Am. J. Physiol. Cell Physiol. **283**:C1228–C1241.
8. **Conboy IM, Conboy MJ, Smythe GM, Rando TA.** 2003. Notch-mediated restoration of regenerative potential to aged muscle. Science **302**:1575–1577.
9. **Conboy IM, et al.** 2005. Rejuvenation of aged progenitor cells by exposure to a young systemic environment. Nature **433**:760–764.
10. **Conboy IM, Rando TA.** 2002. The regulation of Notch signaling controls satellite cell activation and cell fate determination in postnatal myogenesis. Dev. Cell **3**:397–409.
11. **Cornelison DD, et al.** 2004. Essential and separable roles for Syndecan-3 and Syndecan-4 in skeletal muscle development and regeneration. Genes Dev. **18**:2231–2236.
12. **Delfini MC, Hirsinger E, Pourquie O, Duprez D.** 2000. Delta 1-activated notch inhibits muscle differentiation without affecting Myf5 and Pax3 expression in chick limb myogenesis. Development **127**:5213–5224.
13. **Fuentealba L, Carey DJ, Brandan E.** 1999. Antisense inhibition of syndecan-3 expression during skeletal muscle differentiation accelerates myogenesis through a basic fibroblast growth factor-dependent mechanism. J. Biol. Chem. **274**:37876–37884.
14. **Fukada S, et al.** 2011. Hesr1 and Hesr3 are essential to generate undifferentiated quiescent satellite cells and to maintain satellite cell numbers. Development **138**:4609–4619.
15. **Gustafsson MV, et al.** 2005. Hypoxia requires notch signaling to maintain the undifferentiated cell state. Dev. Cell **9**:617–628.
16. **Halevy O, et al.** 2004. Pattern of Pax7 expression during myogenesis in the posthatch chicken establishes a model for satellite cell differentiation and renewal. Dev. Dyn. **231**:489–502.
17. **Jory A, et al.** 2009. Numb promotes an increase in skeletal muscle progenitor cells in the embryonic somite. Stem Cells **27**:2769–2780.
18. **Jouve C, et al.** 2000. Notch signalling is required for cyclic expression of the hairy-like gene HES1 in the presomitic mesoderm. Development **127**:1421–1429.
19. **Kitamoto T, Hanaoka K.** 2010. Notch3 null mutation in mice causes muscle hyperplasia by repetitive muscle regeneration. Stem Cells **28**:2205–2216.
20. **Kopan R, Ilagan MX.** 2009. The canonical Notch signaling pathway: unfolding the activation mechanism. Cell **137**:216–233.
21. **Kopan R, Nye JS, Weintraub H.** 1994. The intracellular domain of mouse Notch: a constitutively activated repressor of myogenesis directed at the basic helix-loop-helix region of MyoD. Development **120**:2385–2396.
22. **Kuang S, Charge SB, Seale P, Huh M, Rudnicki MA.** 2006. Distinct roles for Pax7 and Pax3 in adult regenerative myogenesis. J. Cell Biol. **172**:103–113.
23. **Kuang S, Kuroda K, Le Grand F, Rudnicki MA.** 2007. Asymmetric self-renewal and commitment of satellite stem cells in muscle. Cell **129**:999–1010.
24. **Kuroda K, et al.** 1999. Delta-induced Notch signaling mediated by RBP-J inhibits MyoD expression and myogenesis. J. Biol. Chem. **274**:7238–7244.
25. **Leimeister C, Externbrink A, Klamt B, Gessler M.** 1999. Hey genes: a novel subfamily of hairy- and Enhancer of split-related genes specifically expressed during mouse embryogenesis. Mech. Dev. **85**:173–177.
26. **Lepper C, Conway SJ, Fan CM.** 2009. Adult satellite cells and embryonic muscle progenitors have distinct genetic requirements. Nature **460**:627–631.
27. **Lepper C, Partridge TA, Fan CM.** 2011. An absolute requirement for Pax7-positive satellite cells in acute injury-induced skeletal muscle regeneration. Development **138**:3639–3646.
28. **Mourikis P, et al.** 2012. A critical requirement for Notch signaling in maintenance of the quiescent skeletal muscle stem cell state. Stem Cells **30**:243–252.

29. **Murphy MM, Lawson JA, Mathew SJ, Hutcheson DA, Kardon G.** 2011. Satellite cells, connective tissue fibroblasts and their interactions are crucial for muscle regeneration. Development **138**:3625–3637.
30. **Murtaugh LC, Stanger BZ, Kwan KM, Melton DA.** 2003. Notch signaling controls multiple steps of pancreatic differentiation. Proc. Natl. Acad. Sci. U. S. A. **100**:14920–14925.
31. **Nishijo K, et al.** 2009. Biomarker system for studying muscle, stem cells, and cancer in vivo. FASEB J. **23**:2681–2690.
32. **Olguin HC, Olwin BB.** 2004. Pax-7 up-regulation inhibits myogenesis and cell cycle progression in satellite cells: a potential mechanism for self-renewal. Dev. Biol. **275**:375–388.
33. **Olguin HC, Patzlaff NE, Olwin BB.** 2011. Pax7-FKHR transcriptional activity is enhanced by transcriptionally repressed MyoD. J. Cell. Biochem. **112**:1410–1417.
34. **Olguin HC, Yang Z, Tapscott SJ, Olwin BB.** 2007. Reciprocal inhibition between Pax7 and muscle regulatory factors modulates myogenic cell fate determination. J. Cell Biol. **177**:769–779.
35. **Oustanina S, Hause G, Braun T.** 2004. Pax7 directs postnatal renewal and propagation of myogenic satellite cells but not their specification. EMBO J. **23**:3430–3439.
36. **Pan D, Fujimoto M, Lopes A, Wang YX.** 2009. Twist-1 is a PPARδ-inducible, negative-feedback regulator of PGC-1α in brown fat metabolism. Cell **137**:73–86.
37. **Pisconti A, Cornelison DD, Olguin HC, Antwine TL, Olwin BB.** 2010. Syndecan-3 and Notch cooperate in regulating adult myogenesis. J. Cell Biol. **190**:427–441.
38. **Pourquie O.** 2011. Vertebrate segmentation: from cyclic gene networks to scoliosis. Cell **145**:650–663.
39. **Relaix F, et al.** 2006. Pax3 and Pax7 have distinct and overlapping functions in adult muscle progenitor cells. J. Cell Biol. **172**:91–102.
40. **Rios AC, Serralbo O, Salgado D, Marcelle C.** 2011. Neural crest regulates myogenesis through the transient activation of NOTCH. Nature **473**:532–535.
41. **Rosenblatt JD, Lunt AI, Parry DJ, Partridge TA.** 1995. Culturing satellite cells from living single muscle fiber explants. In Vitro Cell. Dev. Biol. Anim. **31**:773–779.
42. **Sambasivan R, et al.** 2011. Pax7-expressing satellite cells are indispensable for adult skeletal muscle regeneration. Development **138**:3647–3656.
43. **Schultz E, Lipton BH.** 1982. Skeletal muscle satellite cells: changes in proliferation potential as a function of age. Mech. Ageing Dev. **20**:377–383.
44. **Schuster-Gossler K, Cordes R, Gossler A.** 2007. Premature myogenic differentiation and depletion of progenitor cells cause severe muscle hypotrophy in Delta1 mutants. Proc. Natl. Acad. Sci. U. S. A. **104**:537–542.
45. **Schwanbeck R, Martini S, Bernoth K, Just U.** 2011. The Notch signaling pathway: molecular basis of cell context dependency. Eur. J. Cell Biol. **90**:572–581.
46. **Seale P, et al.** 2000. Pax7 is required for the specification of myogenic satellite cells. Cell **102**:777–786.
47. **Shinin V, Gayraud-Morel B, Gomes D, Tajbakhsh S.** 2006. Asymmetric division and cosegregation of template DNA strands in adult muscle satellite cells. Nat. Cell Biol. **8**:677–687.
48. **Song Y, McFarland DC, Velleman SG.** 2011. Role of syndecan-4 side chains in turkey satellite cell growth and development. Dev. Growth Differ. **53**:97–109.
49. **Sun D, Li H, Zolkiewska A.** 2008. The role of Delta-like 1 shedding in muscle cell self-renewal and differentiation. J. Cell Sci. **121**:3815–3823.
50. **Vasyutina E, et al.** 2007. RBP-J (Rbpsuh) is essential to maintain muscle progenitor cells and to generate satellite cells. Proc. Natl. Acad. Sci. U. S. A. **104**:4443–4448.
51. **Waddell JN, et al.** 2010. Dlk1 is necessary for proper skeletal muscle development and regeneration. PLoS One **5**:e15055. doi:10.1371/journal.pone.0015055.
52. **Walker L, et al.** 1999. The Notch/Jagged pathway inhibits proliferation of human hematopoietic progenitors in vitro. Stem Cells **17**:162–171.
53. **Weng AP, et al.** 2006. c-Myc is an important direct target of Notch1 in T-cell acute lymphoblastic leukemia/lymphoma. Genes Dev. **20**:2096–2109.
54. **Wilson-Rawls J, Molkentin JD, Black BL, Olson EN.** 1999. Activated notch inhibits myogenic activity of the MADS-box transcription factor myocyte enhancer factor 2C. Mol. Cell. Biol. **19**:2853–2862.
55. **Zammit PS, et al.** 2004. Muscle satellite cells adopt divergent fates: a mechanism for self-renewal? J. Cell Biol. **166**:347–357.